Supplementary material

## Dysprosium-based complexes with a flat pentadentate donor: a magnetic and ab initio study

Matilde Fondo,[§,] Julio Corredoira-Vázquez,[§] Ana M. García-Deibe,[§] Silvia Gómez-Coca,[£] Eliseo Ruiz,[£] and Jesús Sanmartín-Matalobos[§]*
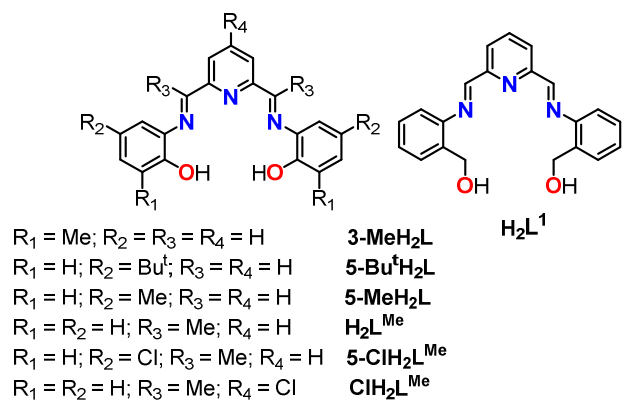
[§] Departamento de Química Inorgánica, Facultade de Química, Universidade de Santiago de Compostela, Campus Vida, 15782 Santiago de Compostela, Spain.

[£] Departament de Química Inorgànica i Orgànica, and Institut de Química Teórica i Computacional, Universitat de Barcelona, 08028 Barcelona, Spain
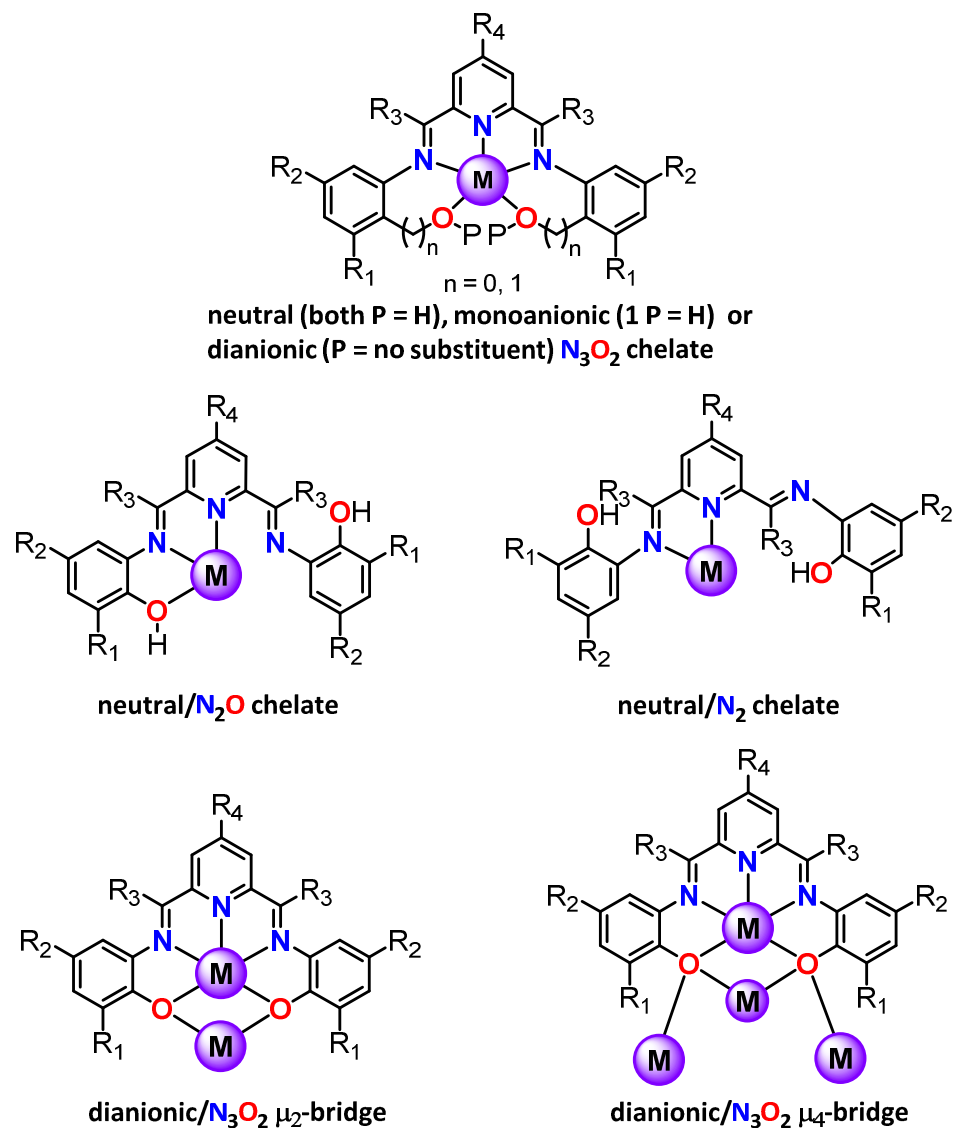
SCHEMES AND FIGURES
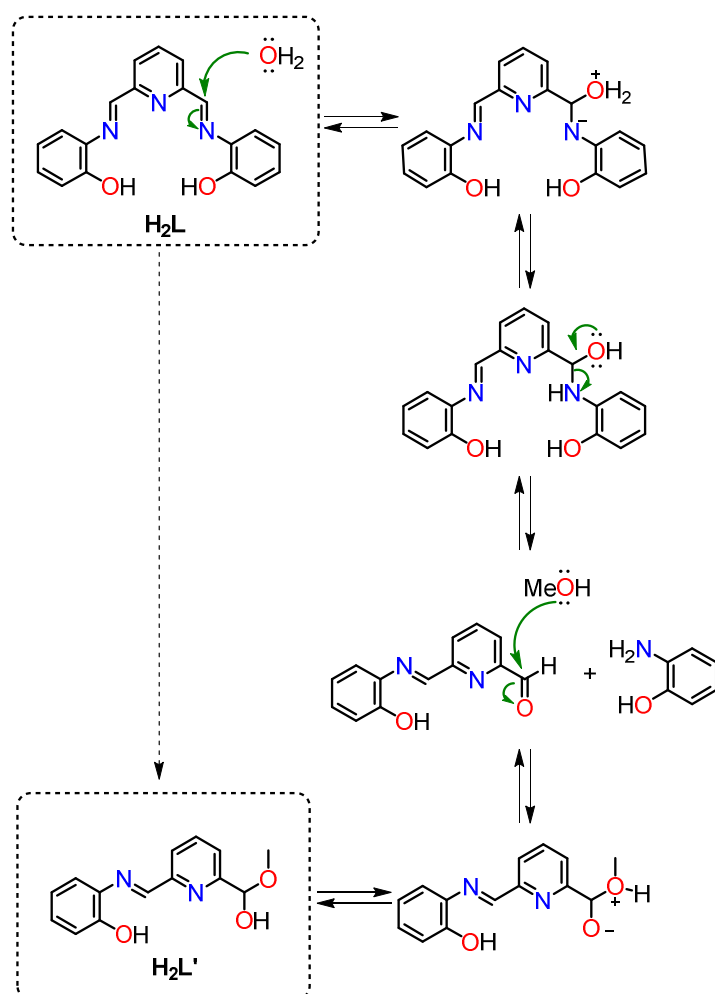
Scheme S1. Proposed mechanism for the formation of hemiacetal from imine functional group

$R_1 = Me$; $R_2 = R_3 = R_4 = H$	**3-MeH$_2$L**
$R_1 = H$; $R_2 = Bu^t$; $R_3 = R_4 = H$	**5-Bu^{t}H$_2$L**
$R_1 = H$; $R_2 = Me$; $R_3 = R_4 = H$	**5-MeH$_2$L**
$R_1 = R_2 = H$; $R_3 = Me$; $R_4 = H$	**H$_2$L^{Me}**
$R_1 = H$; $R_2 = Cl$; $R_3 = Me$; $R_4 = H$	**5-ClH$_2$L^{Me}**
$R_1 = R_2 = H$; $R_3 = Me$; $R_4 = Cl$	**ClH$_2$L^{Me}**

Scheme S2. Related ligands of H$_2$L in crystallographically solved complexes.[14-21] (references in the article)

neutral (both P = H), monoanionic (1 P = H) or dianionic (P = no substituent) N$_3$O$_2$ chelate

neutral/N$_2$O chelate

neutral/N$_2$ chelate

dianionic/N$_3$O$_2$ μ$_2$-bridge

dianionic/N$_3$O$_2$ μ$_4$-bridge

Scheme S3. Coordination modes shown by H$_2$L and the ligands of Scheme S2 in metal complexes.
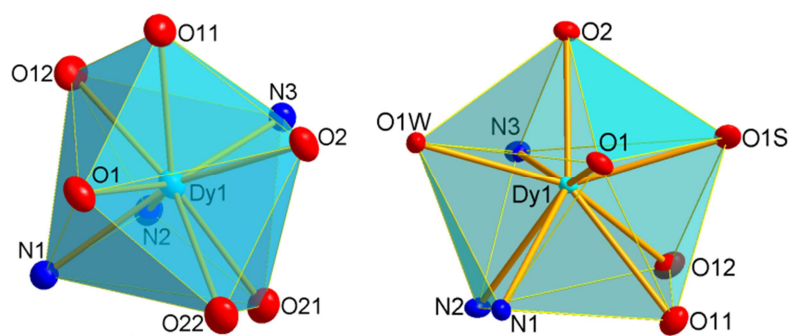
Fig. S1. Coordination environments for the Dy^{III} ions in **1** (left) and **2** (right) showing the distorted spherical tricapped trigonal prism and spherical capped square antiprism structures.
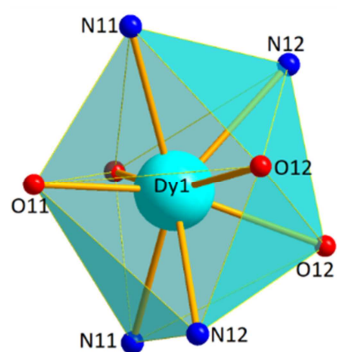

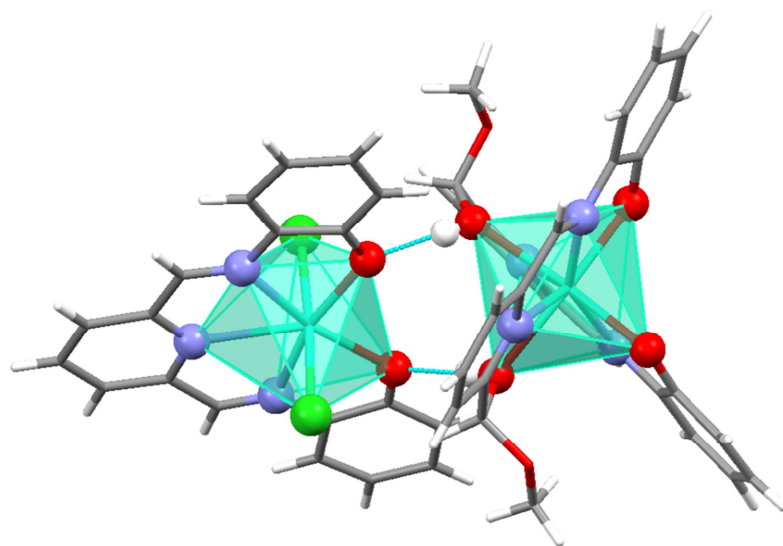**Fig. S2**. Distorted triangular dodecahedron coordination environment for Dy^{III} in **3a**.

Fig. S3. Crystal structure of **3**, showing the hydrogen bond between **3a** and **3b**
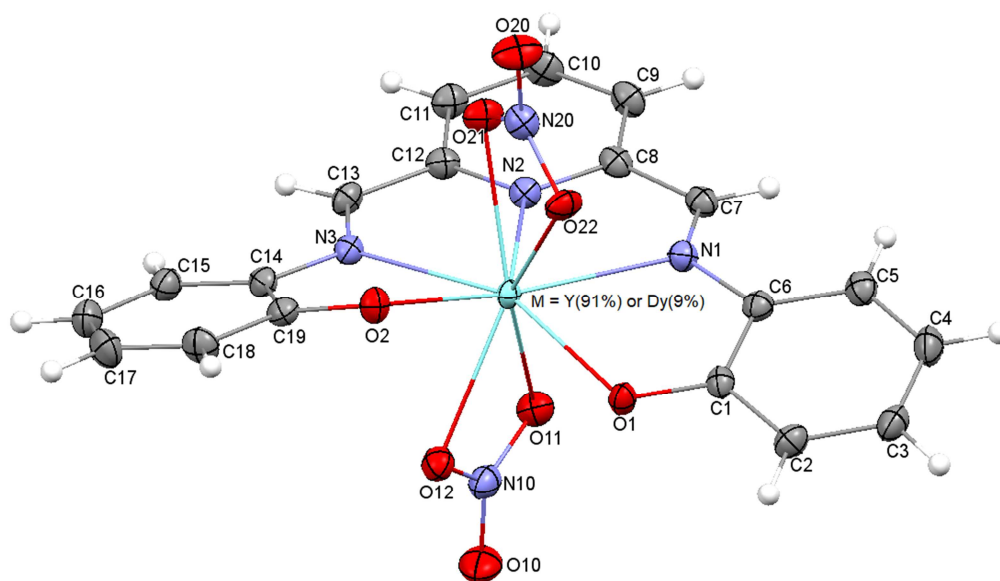
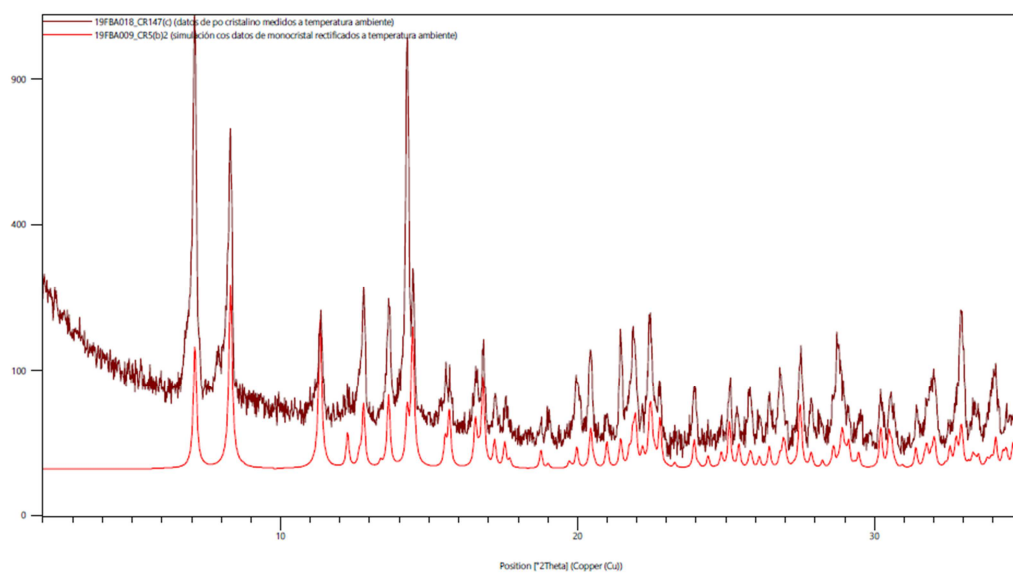**Fig. S4.** Ellipsoid (50% probability) diagram for the anion $[Dy_{0.09}Y_{0.91}(L)(NO_3)_2]^-$ in **4.**

Fig. S5. Comparative powder X-ray diffractograms for **2**·2H$_2$O. Garnet: experimental diffractogram for the microcrystalline sample; red: calculated diffractogram using the data obtained from single X-ray diffraction studies**.**
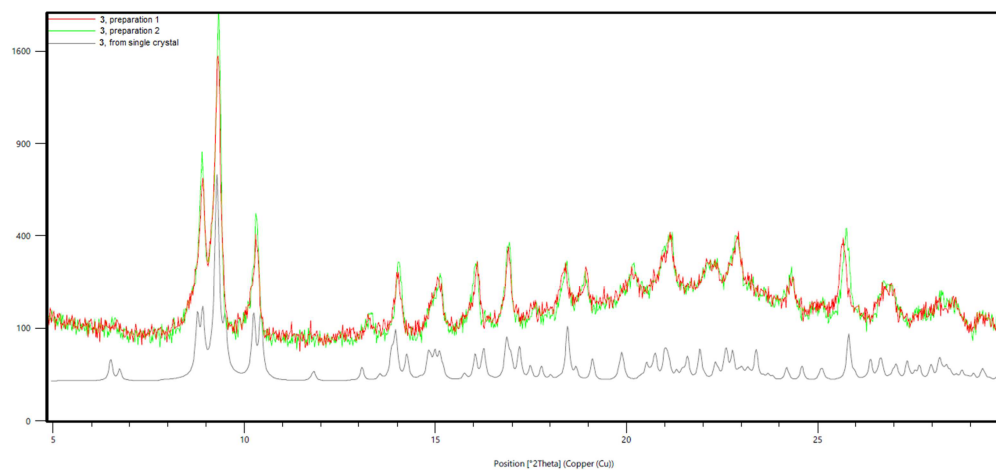
Fig. S6. Comparative powder X-ray diffractograms for **3**: green and red: experimental diffractograms for two microcrystalline samples obtained from two different syntheses; grey: calculated diffractogram using the data obtained from single X-ray diffraction studies**.**
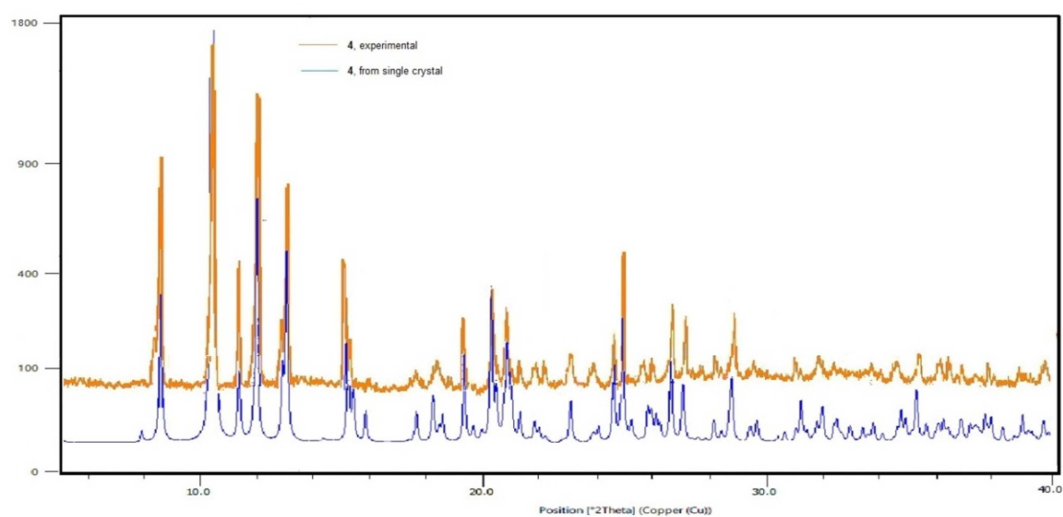
Fig. S7. Comparative powder X-ray diffractograms for **4**. Orange: experimental diffractogram for the microcrystalline sample; blue: calculated diffractogram using the data obtained from single X-ray diffraction studies**.**

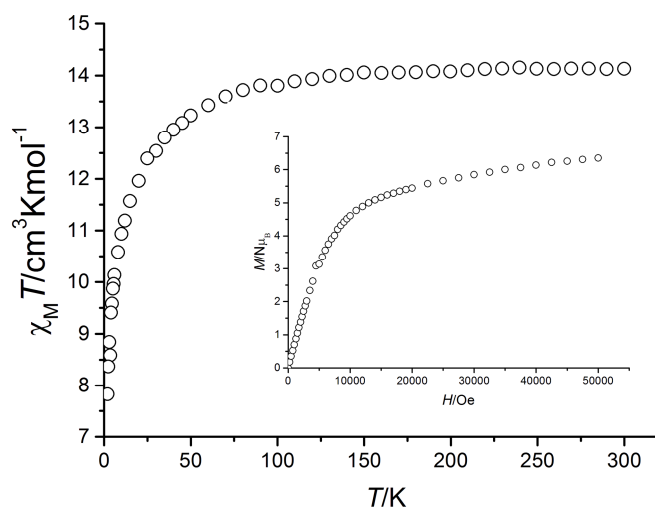**Fig. S8.** $\chi_M T$ *vs T* for **2**·H$_2$O. Inset: *M*/Nμ_B *vs H*.
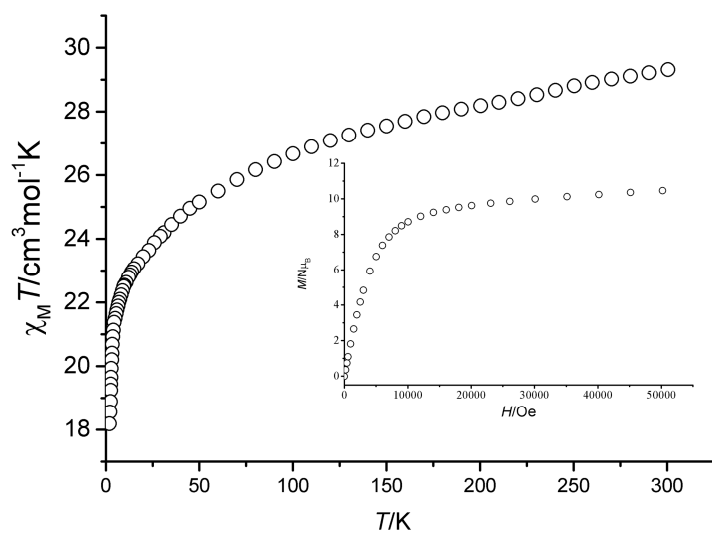
Fig. S9. $\chi_M T$ *vs T* for **3**. Inset: *M*/Nμ_B *vs H*.
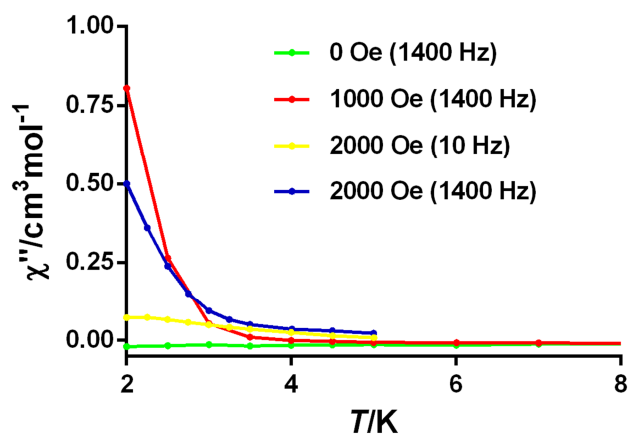
Fig. S10. Temperature, field and frequency dependence of χ_M'' for **1**·H$_2$O
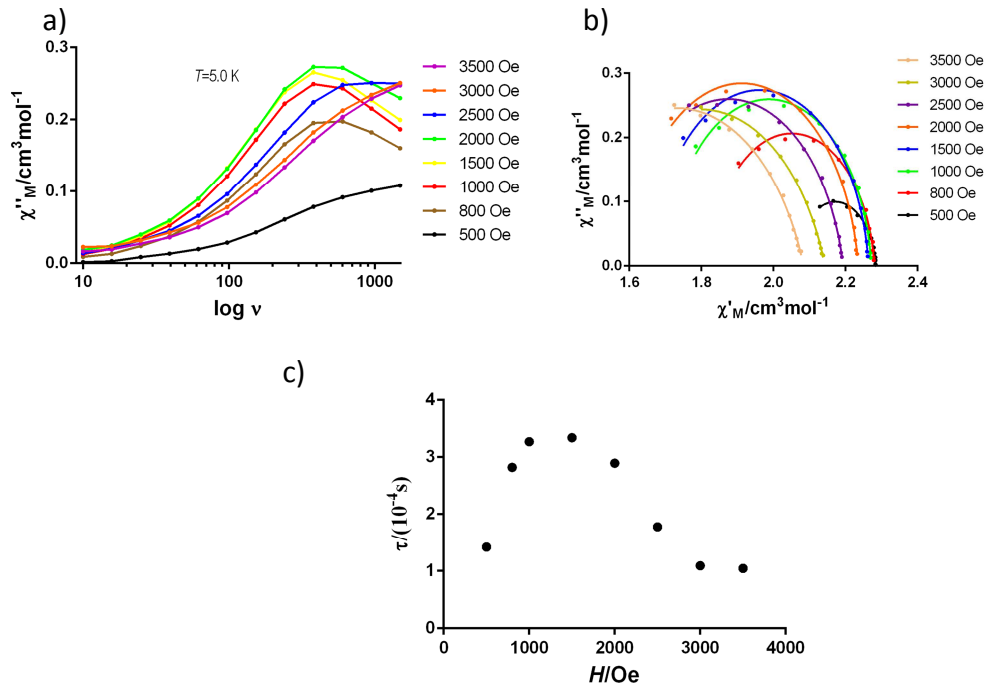
Fig. S11. a) Frequency dependence of χ_M'' for **2**·2H$_2$O at 5 K in various applied fields. b) Cole-Cole plot for **2**·2H$_2$O at 5 K under various applied dc fields. The solid lines represent the best fit of the experimental results with the generalized Debye model. c) Field dependence of the magnetic relaxation time at 5.0 K for **2**·2H$_2$O.
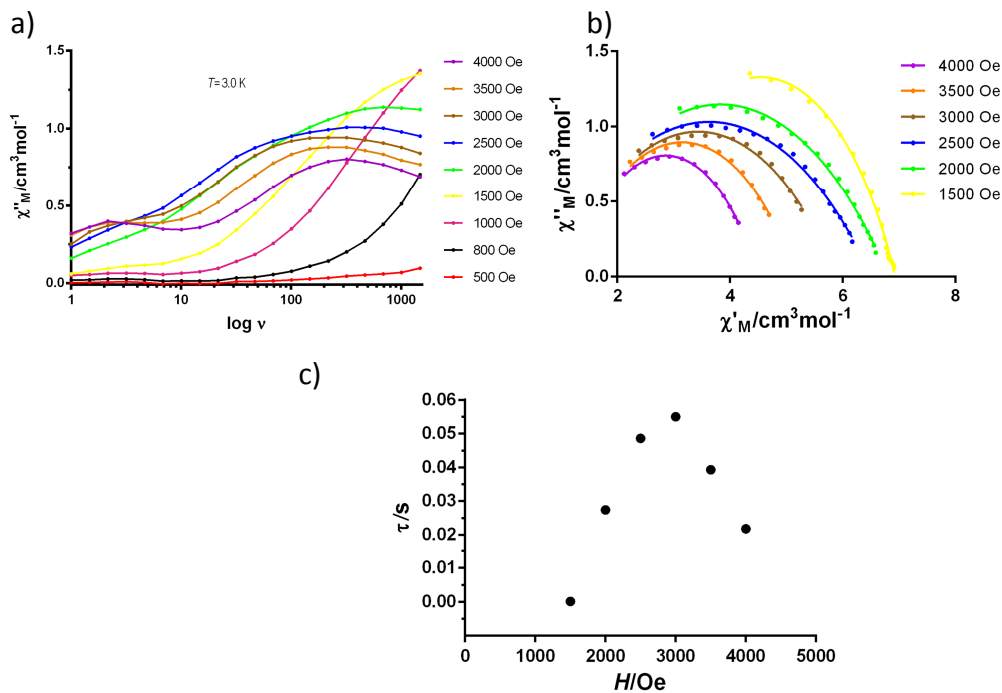
Fig. S12. a) Frequency dependence of χ_M'' for **3** at 3 K in various applied fields. b) Cole-Cole plot for **3** at 3 K under various applied dc fields. The solid lines represent the best fit of the experimental results with the generalized Debye model. c) Field dependence of the magnetic relaxation time at 3.0 K for **3**.
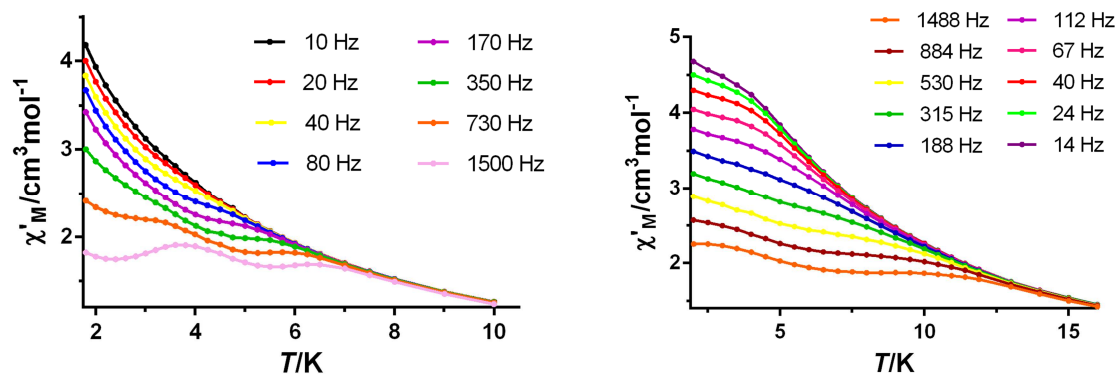
Fig. S13. Temperature dependence of χ'_M for: left) **2**·$2H_2O$ in H_{dc} = 1500 Oe at different frequencies; right) **3** in H_{dc} = 3000 Oe at different frequencies.
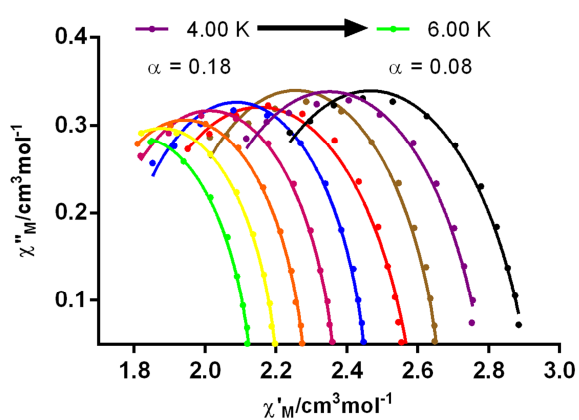
Fig. S14. Cole–Cole plot for **2**·$2H_2O$ in H_{dc} = 1500 Oe.
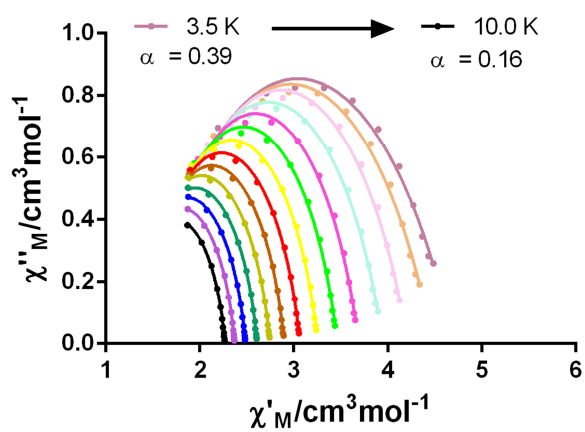
Fig. S15. Cole–Cole plot for **3** in H_{dc} = 3000 Oe.
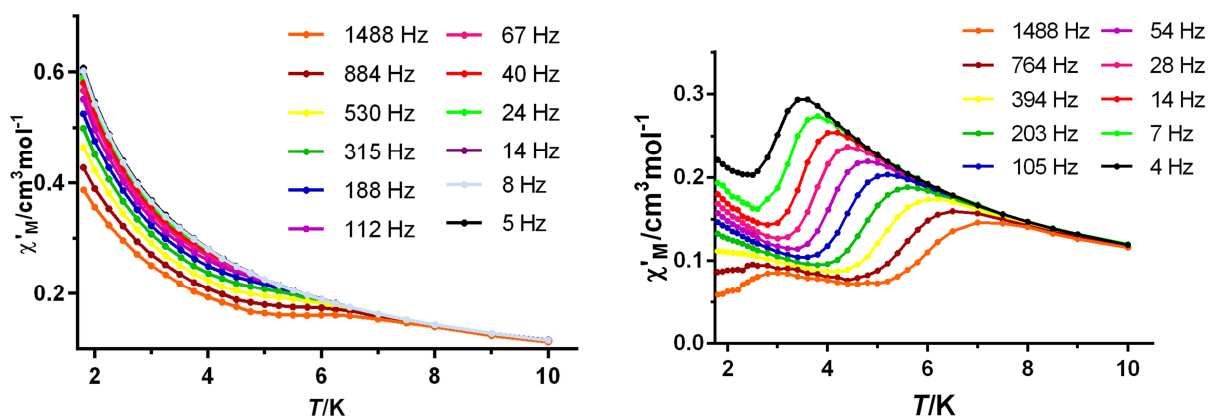
Fig. S16. Temperature dependence of χ'_M for **4** at different frequencies: left) in zero dc field; right) in H_{dc} = 1500 Oe.
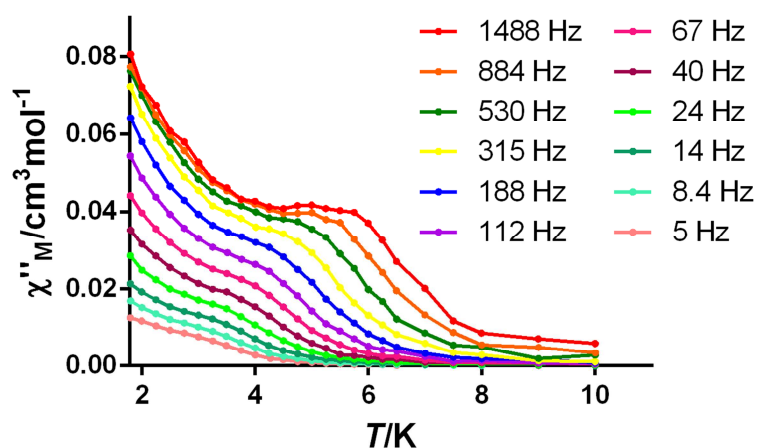
Fig. S17. Temperature dependence of χ''_M for **4** in a dc zero field at different frequencies.
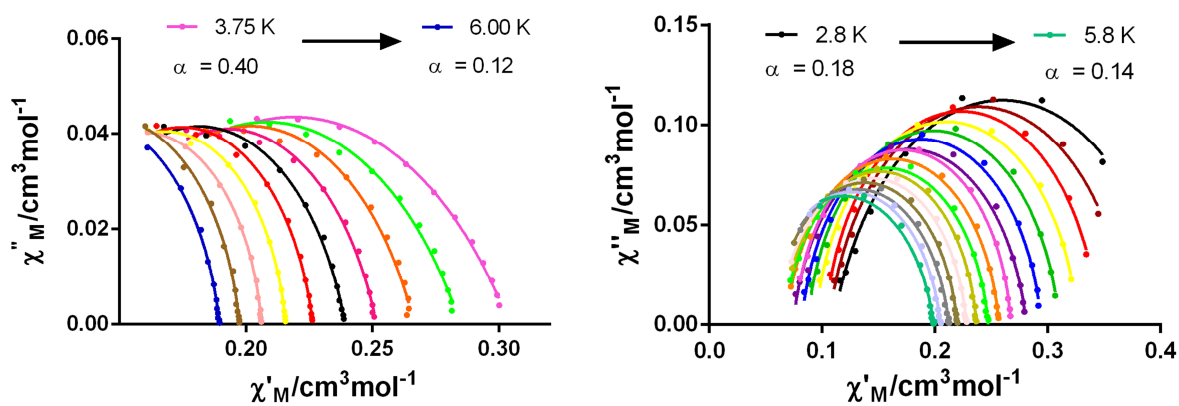
Fig. S18. Cole–Cole plot for **4** in: left) H_{dc} = 0 Oe; right) H_{dc} = 1500 Oe
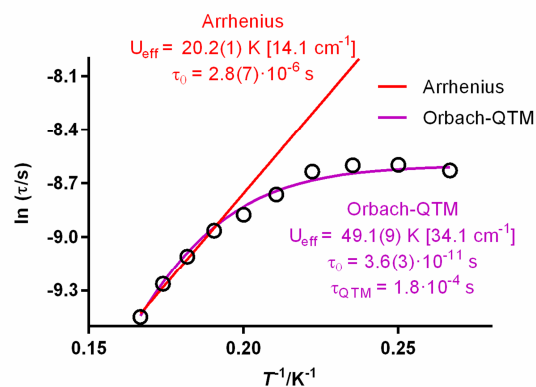
Fig. S19. Arrhenius plot for **4** in a zero dc applied field. The violet line accounts for the best fit considering Orbach plus QTM relaxation (eq. 1 in the article).
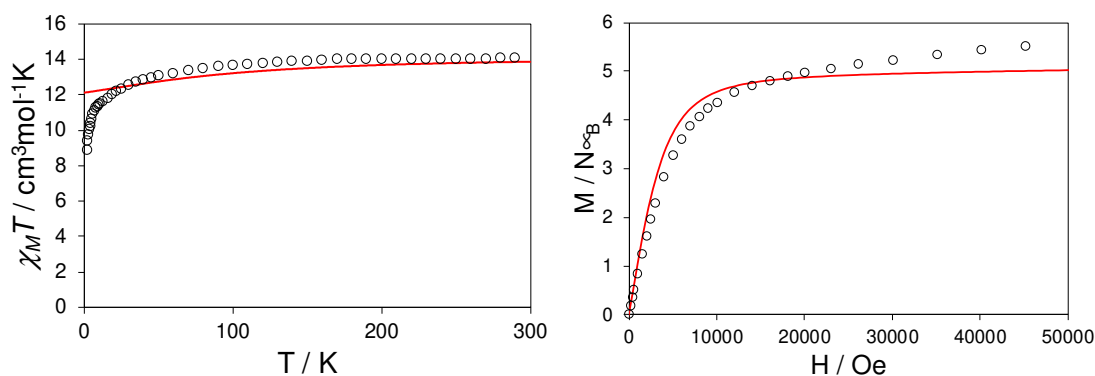
Fig. S20. Comparison between experimental (open circles) and calculated at CASSCF level (red lines) variable temperature dc magnetic susceptibility and magnetization curves for **1** using the model structure for the calculation without including the pyridine molecule (**1wo**).
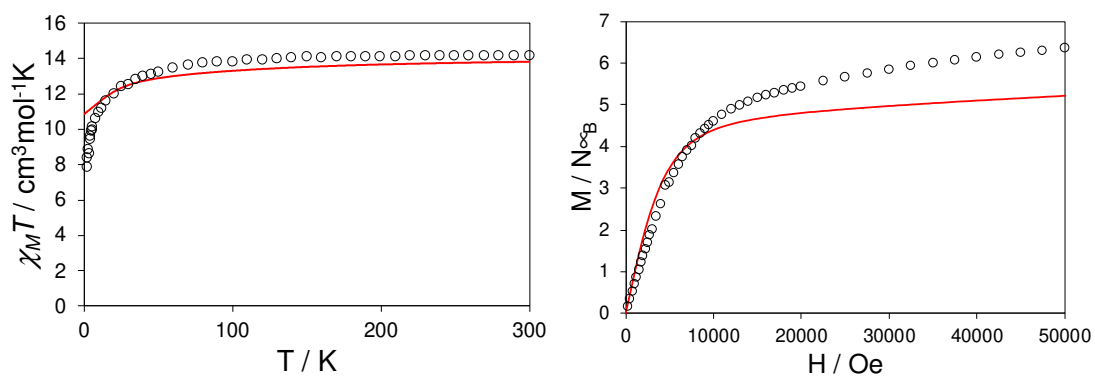
Fig. S21. Comparison between experimental (open circles) and calculated at CASSCF level (red lines) variable temperature dc magnetic susceptibility and magnetization curves for **2**.
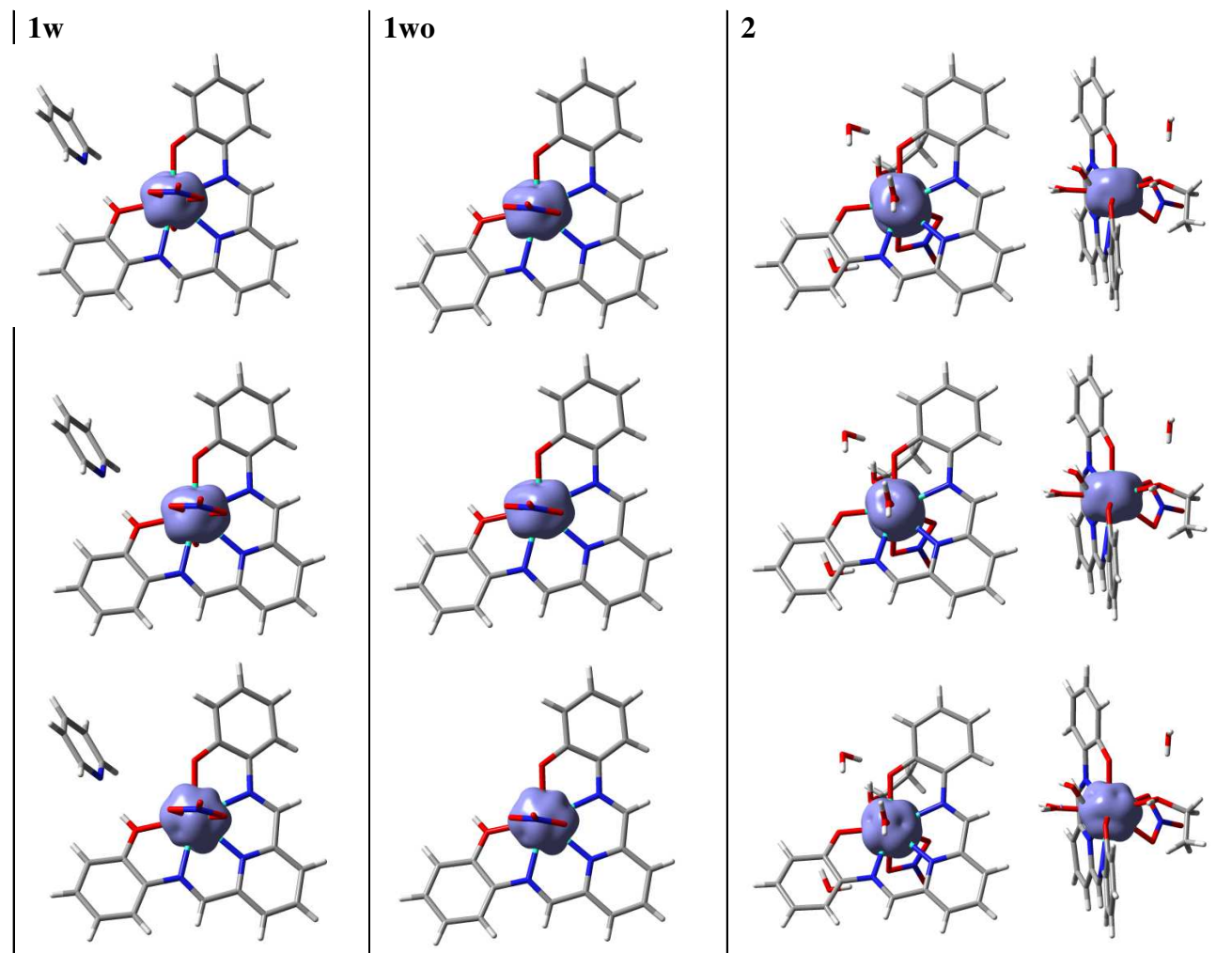
Figure S22. Isosurface of the CASSCF beta electron density of **1w, 1wo** and **2** calculated as the difference between the total density and the sum of the spin density of the seven alpha active electrons for the ground (above), first excited (middle) and second excited (below) states.
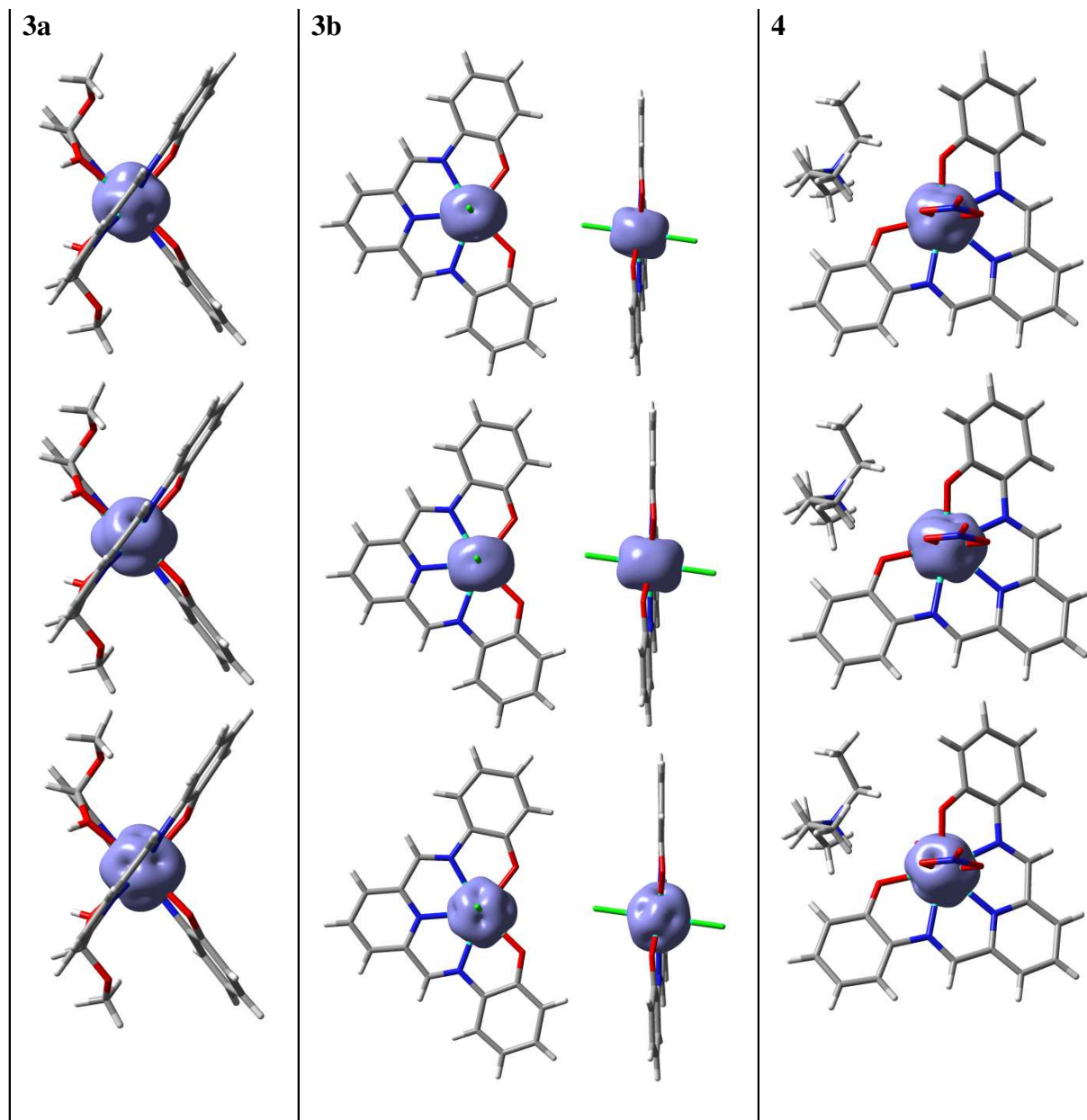
Figure S23. Isosurface of the CASSCF beta electron density of **3a**, **3b** and **4** calculated as the difference between the total density and the sum of the spin density of the seven alpha active electrons for the ground (above), first excited (middle) and second excited (below) states.

TABLES

Table S1. Crystal data and structure refinement for [Dy(HL)(NO$_3$)$_2$]·1.15Py·0.3CH$_3$C$_6$H$_5$ (**1**·1.15Py·0.3CH$_3$C$_6$H$_5$), [Dy(L)(NO$_3$)(H$_2$O)(EtOH)]·2H$_2$O (**2**·2H$_2$O), [Dy(L')$_2$)][Dy(L)(Cl$_2$)] (**3**) and Et$_3$NH[Dy$_{0.1}$Y$_{0.9}$(L)(NO$_3$)$_2$] (**4**).

	1·1.15Py·0.3CH$_3$C$_6$H$_5$	**2**·2H$_2$O	**3**	**4**
Formula	C$_{26.85}$H$_{21.15}$DyN$_{6.15}$O$_8$	C$_{21}$H$_{25}$DyN$_4$O$_9$	C$_{47}$H$_{39}$Cl$_2$Dy$_2$N$_7$O$_8$	C$_{25}$H$_{29}$Dy$_{0.09}$N$_6$O$_8$Y$_{0.91}$
Molecular weight	721.46	639.95	1225.75	637.44
Crystal system	Triclinic	Monoclinic	Monoclinic	Monoclinic
Space group	P-1	$P2_1/n$	$C2/c$	$P2_1/n$
Wavelength (Å)	0.71073	0.71073	0.71073	0.71073
Crystal size (mm^3)	0.180 x 0.040 x 0.020	0.190 x 0.140 x 0.080	0.150 x 0.084 x 0.040	0.080 x 0.060 x 0.020
Color, shape	Red, plate	Red, plate	Red, plate	Orange, prism
T (K)	100(2)	100(2)	100(2)	100(2)
a (Å)	9.8073(10)	13.9344(8)	19.188(4)	10.3588(6)
b (Å)	10.4055(12)	8.2685(5)	18.419(4)	14.8159(10
c (Å)	13.9823(15)	20.4164(11)	12.866(3)	17.2043(11)
α (°)	86.328(4)	90	90	90
β (°)	82.101(4)	100.009(2)	102.517(7)	94.679(3)
γ (°)	74.962(4)	90	90	90
Volume (Å^3)	1364.4(3)	2316.5(2)	4439.2(16)	2631.6(3)
Z	2	4	4	4
Absor. coef. (mm^{-1})	2.800	3.286	3.525	2.337
Reflections collected	74232	179276	13352	61528
Independent reflections	6798 [R_{int} = 0. 0501]	7050[R_{int} = 0. 0367]	6438 [R_{int} = 0.0843]	6517 [R_{int} = 0.1012]
Data / restraints / param.	6798 / 127 / 423	7050 / 6 / 343	6438 / 24 / 289	6517 / 0 / 369
Final R indices [I>2σ(I)]	R_1 = 0.0224 wR_2 = 0.0462	R_1 = 0.0216 wR_2 = 0.0535	R_1 = 0.0765 wR_2 = 0.1940	R_1 = 0.0335 wR_2 = 0.0602
R indices (all data)	R_1 = 0.0277 wR_2 = 0.0486	R_1 = 0.0221 wR_2 = 0.0537	R_1 = 0.1125 wR_2 = 0.2135	R_1 = 0.0581 wR_2 = 0.0681

Table S2. Results of a search in CSD, for crystal structures of Dy[III] complexes contaning ligands with neutral phenol O atoms acting as donors, also including distances for equivalent coordinate phenolate groups, when available.

Journal and the reference	C-O$_{phenol}$	Dy-O$_{phenol}$	C-O$_{phenolate}$	Dy-O$_{phenolate}$
Dalton Trans. 10.1039/C9DT03253C	1.302	2.224		
RSC Advances 10.1039/c6ra16669e	1.299	2.282		
	1.308	2.328		
Dalton Trans. 10.1039/C6DT04027F	1.368	2.646	1.309	2.143
	1.385	2.637	1.322	2.170
CSD Communication CCDC 809223	1.357	2.668	1.321	2.268
J. Coord. Chem. 10.1080/00958972.2012.744002	1.275-1.305	2.264-2.295		
Dalton Trans. 10.1039/c2dt31023f	1.279-1.308	2.311-2.357		
Dalton Trans. 10.1039/a606626g	1.268-1.295	2.254-2.321		
Inorg. Chim. Acta 10.1016/j.ica.2017.08.060	1.346	2.266		
Inorg. Chem. Commun. 10.1016/j.inoche.2014.12.019	1.374-1.378	2.400-2.438		
Dalton Trans. 10.1039/c2dt11539e	1.279	2.252		
Eur. J. Inorg. Chem. 10.1002/ejic.201201336	1.297	2.309		
Dalton Trans. 10.1039/C5DT02563J	1.386-1.401	2.477-2.481		
This work	1.354	2.366	1.325	2.239

Table S3. Main bond distances (Å) and angles for **1**·1.15Py·0.3CH$_3$C$_6$H$_5$ and **2**·2H$_2$O.

	1·1.15Py·0.3CH$_3$C$_6$H$_5$	**2**·2H$_2$O
Dy1-O1	2.2391(16)	2.2689(17)
Dy1-O2	2.3663(16)	2.2869(17)
Dy1-N2	2.4872(19)	2.503(2)
Dy1-N1	2.4713(19)	2.529(2)
Dy1-N3	2.4971(19)	2.538(2)
Dy1-O11	2.4445(17)	2.5201(19)
Dy1-O12	2.4570(18)	2.5691(19)
Dy1-O21	2.4576(18)	
Dy-O1W		2.3723(18)
Dy1-O22	2.4944(15)	
Dy-O1S		2.578(11)
O11-Dy1-O12		50.22(6)
O21-Dy1-O22	51.64(7)	
O1-Dy1-N3	158.34(6)	160.12(6)

Table S4. SHAPE v2.1. Continuous Shape Measures calculation (c) 2013 Electronic Structure Group, Universitat de Barcelona

Geometries Coordination number 9

MFF-9   13 Cs   Muffin
HH-9   12 C2v   Hula-hoop
JTDIC-9   11 C3v   Tridiminished icosahedron J63
TCTPR-9   10 D3h   Spherical tricapped trigonal prism
JTCTPR-9   9 D3h   Tricapped trigonal prism J51
CSAPR-9   8 C4v   Spherical capped square antiprism
JCSAPR-9   7 C4v   Capped square antiprism J10
CCU-9   6 C4v   Spherical-relaxed capped cube
JCCU-9   5 C4v   Capped cube J8
JTC-9   4 C3v   Johnson triangular cupola J3
HBPY-9   3 D7h   Heptagonal bipyramid
OPY-9   2 C8v   Octagonal pyramid
EP-9   1 D9h   Enneagon

Geometries Coordination number 8

TBPY-8   13 D3h   Elongated trigonal bipyramid
TT-8   12 Td   Triakis tetrahedron
JSD-8   11 D2d   Snub diphenoid J84
BTPR-8   10 C2v   Biaugmented trigonal prism
JBTPR-8   9 C2v   Biaugmented trigonal prism J50
JETBPY-8   8 D3h   Johnson elongated triangular bipyramid J14
JGBF-8   7 D2d   Johnson gyrobifastigium J26
TDD-8   6 D2d   Triangular dodecahedron
SAPR-8   5 D4d   Square antiprism
CU-8   4 Oh   Cube
HBPY-8   D6h   Hexagonal bipyramid
HPY-8   2 C7v   Heptagonal pyramid
OP-8   1 D8h   Octagon

Geometries Coordination number 7

ETPY-7   7 C3v   Johnson elongated triangular pyramid J7
JPBPY-7   6 D5h   Johnson pentagonal bipyramid J13
CTPR-7   5 C2v   Capped trigonal prism
COC-7   4 C3v   Capped octahedron
PBPY-7   3 D5h   Pentagonal bipyramid
HPY-7   2 C6v   Hexagonal pyramid
HP-7   1 D7h   Heptagon

1·1.15Py·0.3CH$_3$C$_6$H$_5$

Structure [ML9]		**MFF-9**	HH-9	JTDIC-9	**TCTPR-9**	JTCTPR-9	CSAPR-9
		3.139,	8.701,	10.396,	**2.699**,	4.195,	3.334,
JCSAPR-9	CCU-9	JCCU-9	JTC-9	HBPY-9	OPY-9	EP-9	
4.331,	4.782,	6.504,	16.000,	16.280,	21.730,	36.402	

2·2H$_2$O

Structure [ML9]	**MFF-9**	HH-9	JTDIC-9	TCTPR-9	JTCTPR-9	**CSAPR-9**
	2.012,	8.895,	10.756,	2.863,	4.393,	**1.909,**
JCSAPR-9	CCU-9	JCCU-9	JTC-9	HBPY-9	OPY-9	EP-9
2.680,	5.410,	6.596,	15.941,	15.998,	24.017,	36.365

3

3a

Structure [ML8]	ETBPY-8	TT-8	JSD-8	BTPR-8	JBTPR-8	JETBPY-8	JGBF-8
	20.878,	10.340,	**2.888**,	3.649,	3.760,	23.682	9.730

TDD-8	SAPR-8	CU-8	HBPY-8	HPY-8	OP-8
2.836,	4.306,	9.495,	12.407,	24.894,	32.855

3b

Structure [ML7]	JETPY-7	JPBPY-7	CTPR-7	COC-7	**PBPY-7**	HPY-7	HP-7
	19.934,	6.452,	5.941,	8.093,	**1.345**,	23.284,	33.054

4

Y

Structure [ML9]	**MFF-9**	HH-9	JTDIC-9	**TCTPR-9**	JTCTPR-9	CSAPR-9
	2.734,	9.476,	10.259,	**2.290**,	3.873,	2.954,

JCSAPR-9	CCU-9	JCCU-9	JTC-9	HBPY-9	OPY-9	EP-9
3.832,	5.518,	7.256,	15.793,	16.574,	20.951,	36.788

Dy

Structure [ML9]	**MFF-9**	HH-9	JTDIC-9	**TCTPR-9**	JTCTPR-9	CSAPR-9
	2.715,	9.535,	10.269,	**2.308**,	3.891,	2.973

JCSAPR-9	CCU-9	JCCU-9	JTC-9	HBPY-9	OPY-9	EP-9
3.981,	5.535,	7.276,	15.836,	16.589,	20.967,	36.799

Table S5. Main bond distances (Å) and angles (°) for **3**.

3a		3b	
Dy1-O11	2.219(9)	Dy2-O21	2.286(9)
Dy1-O12	2.408(10)	Dy2-Cl2	2.615(3)
Dy1-N11	2.452(11)	Dy2-N21	2.506(10)
Dy1-N12	2.488(10)	Dy2-N22	2.480(15)
O12-Dy1-N12	64.0(3)	N22-Dy2-N21	64.9(3)
O11-Dy1-O12	162.5(3)	Cl2-Dy2-Cl2[#1]	176.74(16)

#1: -x+1,y,-z+3/2

Table S6. Main bond distances (Å) and angles (º) for **4**

Y1-O2	2.251(3)	Dy1-O2	2.226(13)
Y1-O1	2.288(3)	Dy1-O1	2.322(13)
Y1-O12	2.465(3)	Dy1-O12	2.352(12)
Y1-O11	2.470(3)	Dy1-O11	2.384(12)
Y1-O21	2.471(3)	Dy1-O21	2.556(12)
Y1-O22	2.442(3)	Dy1-O22	2.558(12)
Y1-N1	2.479(3)	Dy1-N1	2.554(13)
Y1-N3	2.493(3)	Dy1-N3	2.418(13)
Y1-N2	2.507(3)	Dy1-N2	2.508(13)
O2-Y1-N1	158.24(13)	O1-Dy1-N3	161.2(6)
O22-Y1-O21	52.12(7)	O21-Dy1-O22	49.9(2)

Table S7. Metal complexes derived from H_2L and related ligands crystallographically solved.

Metal complex[a]	Charge/ Coordination mode[b]	Nuclearity	Ref. in the article
$[Cd_3L(OAc)_2(dmf)_2]$	dianionic/ N_3O_2 μ_2-bridge	trinuclear	14
$[ReL(PPh_3)_2]I$	dianionic/ N_3O_2 chelate	mononuclear	15
fac-$[Re(CO)_3H_2L(Br)]$	neutral/ N_2 chelate	mononuclear	15
fac-$[Re(CO)_3H_2L(Cl)]$	neutral/ N_2 chelate	mononuclear	16
$[SnL(Bu^n)_2]$	dianionic/ N_3O_2 chelate	mononuclear	13
$[SnL(Ph)_2]$	dianionic/ N_3O_2 chelate	mononuclear	13
$[Mn(H_2L)Cl_2]$	neutral/ N_3O_2 chelate	mononuclear	17
$[Mn_2Ca(L)_2(OAc)_2(MeOH)_2]$	dianionic/ N_3O_2 μ_2-bridge	trinuclear	17
$[Mn_3(L)_2(OAc)_2(MeOH)_2]$	dianionic/ N_3O_2 μ_2-bridge	trinuclear	17
$[Zn_2(L)(OAc)_2(DMF)]$	dianionic/ N_3O_2 μ_2-bridge	dinuclear	18
$[Zn_4(5-Bu^tL)_2(OAc)_4]$	dianionic/ N_3O_2 μ_4-bridge	tetranuclear	18
$[Zn(3-MeH_2L)(Cl)_2]$	neutral/ N_2O chelate	mononuclear	19
$[Zn_2(5-MeL)(Cl)_2(MeOH)_2]$	dianionic/ N_3O_2 μ_2-bridge	dinuclear	19
$[Mn(5-MeHL)(Cl)(MeOH)]$	monoanionic/ N_3O_2 chelate	mononuclear	20
$[Sn(5-MeL)(Bu^n)_2]$	dianionic/ N_3O_2 chelate	mononuclear	13
$[Mn(H_2L^1)(NCS)_2]$	neutral/ N_3O_2 chelate	mononuclear	20
$[Cd_4(L^{Me})_2(OAc)_4]$	dianionic/ N_3O_2 μ_4-bridge	tetranuclear	14,18
$[Sn(L^{Me})(Bu^n)_2]$	dianionic/ N_3O_2 chelate	mononuclear	13
$[Sn(L^{Me})(Me)_2]$	dianionic/ N_3O_2 chelate	mononuclear	13
$[Mn_4(L^{Me})_2(OAc)_4]$	dianionic/ N_3O_2 μ_4-bridge	tetranuclear	21
$[Mn_4(L^{Me})_2(CF_3COO)_4]$	dianionic/ N_3O_2 μ_4-bridge	tetranuclear	21
$[Zn_4(L^{Me})_2(OAc)_4]$	dianionic/ N_3O_2 μ_4-bridge	tetranuclear	18
$[Zn_4(L^{Me})_2(OAc)(O_2CC_6H_5)_3]$	dianionic/ N_3O_2 μ_4-bridge	tetranuclear	18
$[Zn_4(5-ClL^{Me})_2(OAc)_4]$	dianionic/ N_3O_2 μ_4-bridge	tetranuclear	18

[a] Complexes without solvates; ligands in Scheme S2 (except H_2L, Scheme 1); [b] coordination mode in Scheme S3

Table S8. Generalised Debye model fitting parameters for **2·2H$_2$O-4**

Compounds	T/K	χ_S/(cm^{3}mol^{-1})	χ_T/(cm^{3}mol^{-1})	τ/(10^{-4}s)	α
2·2H$_2$O	4.00	2.01	2.92	10.64	0.18
	4.25	1.91	2.79	7.05	0.17
	4.50	1.85	2.67	5.36	0.12
	4.75	1.72	2.59	4.01	0.19
	5.00	1.72	2.46	2.97	0.08
	5.25	1.66	2.37	2.35	0.07
	5.50	1.47	2.07	1.80	0.08
	5.75	1.55	2.21	1.31	0.06
	6.0	1.49	2.13	0.95	0.08
3	3.5	1.39	4.70	5.01	0.39
	4.0	1.45	4.48	5.01	0.36
	4.5	1.51	4.21	4.88	0.31
	5.0	1.51	3.95	4.54	0.28
	5.5	1.50	3.69	4.09	0.24
	6.0	1.47	3.46	3.52	0.22
	6.5	1.42	3.25	3.00	0.21
	7.0	1.40	3.07	2.57	0.19
	7.5	1.36	2.90	2.11	0.18
	8.0	1.30	2.75	1.78	0.18
	8.5	1.30	2.61	1.44	0.17
	9.0	1.26	2.48	1.25	0.17
	9.5	1.25	2.37	1.04	0.16
	10	1.24	2.27	0.89	0.16
4 (H$_{dc}$=0 Oe)	3.75	0.13	0.30	1.79	0.40
	4.00	0.13	0.28	1.85	0.35
	4.25	0.14	0.27	1.84	0.27
	4.50	0.13	0.25	1.78	0.23
	4.75	0.12	0.24	1.57	0.20
	5.00	0.12	0.23	1.40	0.14
	5.25	0.12	0.22	1.28	0.10
	5.50	0.11	0.21	1.11	0.09
	5.75	0.094	0.20	0.95	0.11
	6.00	0.084	0.19	0.79	0.12
4 (H$_{dc}$=1500 Oe)	2.8	0.11	0.41	595	0.18
	3.0	0.11	0.37	358	0.13
	3.2	0.10	0.35	223	0.08
	3.4	0.094	0.33	138	0.09
	3.6	0.087	0.31	87.5	0.09
	3.8	0.082	0.29	55.3	0.09
	4.0	0.074	0.28	35.5	0.10
	4.2	0.076	0.27	23.9	0.06
	4.4	0.068	0.26	16.2	0.08
	4.6	0.066	0.25	11.4	0.09
	4.8	0.065	0.24	7.91	0.07
	5.	0.062	0.23	5.76	0.08
	5.2	0.056	0.22	4.10	0.09
	5.4	0.052	0.21	3.05	0.11
	5.6	0.047	0.20	2.23	0.11
	5.8	0.039	0.20	1.79	0.14